MECHANISM AND EXPERIMENTAL STUDY OF BIMETALLIC SOLID CATALYSTS ON UREA CATALYTIC HYDROLYSIS TO AMMONIA

Xiangyu ZHANG[a], Hainan WEN[b], Shiming XU[b], Zhihua DU[c], Zhaoyao MA[b], Xiaofeng XIANG[a], Zhichao WANG[a]

[a] Xi'an Thermal Power Research Institute CO., Ltd, Xi'an, Shaanxi, China

[b] School of Low-Carbon Energy and Power Engineering, China University of Mining and Technology, Xuzhou, Jiangsu, China

[c] School of Energy and Power Engineering, Xi'an Jiaotong University, Xi'an, Shaanxi, China

*Corresponding authors: *zhangxiangyu214@163.com*

In order to solve the problems of slow reaction rate and large reactor volume of traditional urea hydrolysis to ammonia, the urea catalytic hydrolysis was studied in this paper. The bimetallic solid catalyst TiO_2@Al_2O_3 was synthesized firstly, in which the mesoporous γ-Al_2O_3 was selected as substrate and the TiO_2 was inserted into the active site. The solid catalyst was characterized by Raman spectroscopy and TEM, and the intermediates were qualitatively detected by liquid NMR H-spectroscopy and C-spectroscopy, which was combined with DFT calculations to analysis the mechanism of the bimetallic solid catalyst. And then, the kinetic and thermodynamic properties of the urea catalytic hydrolysis by solid catalyst were investigated on a batch reactor and a continuous operation pilot plant. The kinetic parameters of the catalytic hydrolysis reaction were measured, and the influences of different catalysts on the hydrolysis reaction temperature, energy consumption and variable load response time were researched. The bimetallic solid catalyst proposed in this study can solve the problems of phosphorus-containing wastewater discharge and insufficient active sites of traditional catalysts, and will provide significant reference to the research of urea catalytic hydrolysis to ammonia for flue gas denitrification.

Key word: *urea catalytic hydrolysis; bimetallic; solid catalysts; ammonia; denitrification*

1. Introduction

The reaction of urea hydrolysis to ammonia under specific temperatures and pressures can be simplified to two steps [1]. Firstly, the urea reacts with water to generate ammonium carbamate, then the ammonium carbamate is thermally decomposed to generate ammonia and carbon dioxide, which is a strong endothermic reaction, as shown in eq. (1)-(2):

$$NH_2CONH_2 + H_2O \rightarrow NH_2COONH_4 \quad (1)$$

$$NH_2COONH_4 \rightarrow 2NH_3 + CO_2 \quad (2)$$

The traditional urea hydrolysis processes faced with some challenges due to the low reaction temperature, such as slow reaction rate, large reactor volume and long response time to variable loads [2]. In order to improve the conversion and reaction rate of urea hydrolysis to ammonia, some scholars had proposed the urea catalytic hydrolysis process, in which the catalysts were used to reduce the activation energy required for the reaction, to shorten the equilibrium time of the reversible reaction, so as to accelerate the hydrolysis rate of urea and improve the production rate of ammonia [3]. The polyphosphates such as ammonium dihydrogen phosphate and diammonium hydrogen phosphate were commonly used as liquid catalyst for urea catalytic hydrolysis, it participates in the reaction as a Lewis acid [4]. Young [5] used inorganic acids as catalysts to catalyze urea hydrolysis to produce ammonia in his patent, it can obtain high-purity NH_3, but the liquid acids can seriously corrode the reaction equipment. In addition, the liquid phosphate catalyst is difficult to recycle, and the phosphorus containing in the reaction solution will increase the cost of wastewater treatment [6].

The urea decomposition to ammonia is affected by the alkalinity and the alkali amount on the catalyst surface, so the solid alkali metal oxides can be selected to be the catalytic to accelerate the hydrolysis reaction rate of urea [7]. The urea degradation efficiency can reach to 58% at 383 K when using the vanadium compounds as catalyst [8]. The urea degradation efficiency can reach to 80% within 30 min at 449 K when using the metal chromium oxides. The palladium compounds are able to complex with urea molecules and to promote the urea decomposition when the pH is 3.3. Other metal oxides such as MnO_2, MoO_3, Cr_2O_3 and Al_2O_3 also showed positive catalytic effects to urea hydrolysis [9].

The urea catalytic hydrolysis to ammonia has been applied in industry, but there is still some debate about its practical role and economic viability. Some researchers believe that the addition of catalysts can accelerate the variable load response time, lower the hydrolysis reaction temperature, reduce the acid corrosion, and improve the urea decomposition rate [10]. However, some researchers have questioned that the catalytic hydrolysis does not significantly reduce the reaction temperature and pressure, and the corrosion of reactor may be increased due to the acidity of the catalyst [11]. On the other hand, the influence of catalyst addition on the kinetics is still not clear, and it is necessary to study the mechanism and reaction characteristics of catalytic hydrolysis of urea.

The phosphate catalysts would cause phosphorus discharge in wastewater, while the single metal oxide catalysts are difficult to generate effective active sites due to the stable surface coordination structure [12]. In this paper, a bimetallic composite oxide was designed as the catalyst for urea hydrolysis reaction, the kinetic and thermodynamic properties of urea catalytic hydrolysis were investigated by using a batch reactor and a continuous operation pilot plant, and the relevant conclusions will provide a reference for the design of urea catalytic hydrolysis process.

2. Catalyst Preparation and Characterization

2.1. Preparation of the catalysts

The Al_2O_3 hydrate can form relatively stable L acid center and L base center (O^{2-}) after calcination and dehydration, and the alkaline earth metal oxide TiO_2 has a large amount of O^{2-} and a small part of OH on its surface, thus the two metal oxides can be combined to be a composite catalyst as that the L base center is able to provide electron pairs to promote the C-N bond breaking [13]. The mesoporous γ-Al_2O_3 (CAS number: 1344-28-1) was chosen as substrate, by loading nano-sized TiO_2

(CAS number: 13463-67-7) to synthesize bimetallic solid metal oxides TiO_2@Al_2O_3 as catalysts for urea hydrolysis.

The synthetic method of TiO_2@Al_2O_3 is as follows:

(1) According to the set molar ratio of Ti/Al, different weights of TiO_2 and mesoporous γ-Al_2O_3 particles are weighed and mixed.

(2) Add some deionized water, and the ultrasonic and stirring treatment is utilized to generate suspensions containing TiO_2 and mesoporous γ-Al_2O_3.

(3) Separate the solid and liquid in the suspension by centrifuge, then the precipitate is dried at a constant temperature of 373 K for 6h and calcined at 773 K for 4 h.

(4) The TiO_2@Al_2O_3 catalyst is obtained by grinding the products until it could pass through 150 sieves.

The Raman spectra of the catalysts were tested under 532 nm laser excitation. The results are shown in Fig. 1, which indicated that TiO_2 has been loaded into mesoporous γ-Al_2O_3. As we can see, the Raman peaks of TiO_2 appear at 636 cm^{-1}, 514 cm^{-1}, 394 cm^{-1}, 194 cm^{-1} and 142 cm^{-1}, which represents different Raman vibrational modes. The peak at 142 cm^{-1} is caused by the planar bending vibration of the O-Ti-O bond, and the peak at 636 cm^{-1} is caused by the telescopic vibration of the Ti-O bond. No significant Raman signal was detected for mesoporous γ-Al_2O_3. The peak position of the Raman displacement signal for TiO_2@Al_2O_3 is basically consistent with TiO_2, but the intensity is slightly lower.

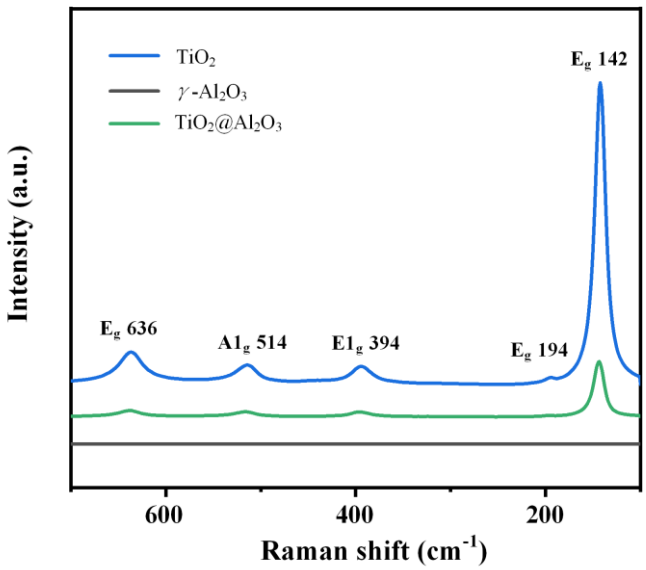

Fig. 1. Raman spectroscopy test results of catalysts

The TEM (Transmission Electron Microscopy) was used to accurately observe the micro-morphological characteristics of the catalyst, the test results are shown in Fig. 2. The morphology of TiO_2@Al_2O_3 can be observed by low magnification projection, and the material is spotted as a whole and flocculent locally. The dark spots are agglomerates loaded with TiO_2, and the strips of flocculent are mesoporous Al_2O_3. The EDX (Energy-dispersive X-ray spectroscopy) was used to scan the element in the observation area, and the elements Ti, Al and O are detected, whose distribution areas were consistent with the material structure, further confirming that TiO_2 is loaded onto the surface of Al_2O_3. As observed in the local morphology of the catalyst, the edge region of the

material is a crystal region with good crystallinity (the red dashed box part of Fig. 2c), which is presumed to be TiO_2 nanocluster. The high magnification TEM results are shown in Fig. 2d. The yellow dashed area has good crystallinity and a lattice spacing of 3.52 Å, belonging to the (101) crystal plane of rutile TiO_2. The crystallinity around TiO_2 is relatively poor, and the lattice fringe spacing in the crystal structure region (red dotted box) is 2.05 Å, belonging to the (400) crystal plane of mesoporous γ-Al_2O_3.

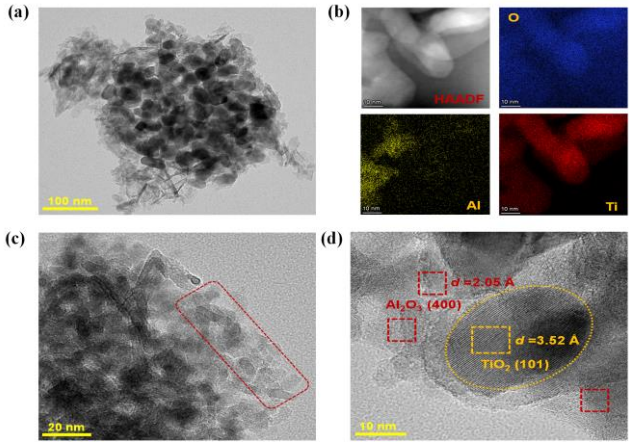

Fig. 2. TEM test results of TiO_2@Al_2O_3

Low magnification (a); Element distribution (b); Local morphology (c); Lattice fringe

The specific surface area, pore area, pore volume and pore size of the catalyst were measured by physical adsorption instrument, The results are shown in Table. 1. The specific surface areas of TiO_2 and mesoporous γ-Al_2O_3 are 76.5 $m^2 \cdot g^{-1}$, 85.1 $m^2 \cdot g^{-1}$, respectively, and the pore surface area, pore volume and average pore size of mesoporous γ-Al_2O_3 are higher than those of TiO_2. The specific surface area, pore area, average pore volume and pore size of TiO_2@Al_2O_3 are 152.1 $m^2 \cdot g^{-1}$, 170.7 $m^2 \cdot g^{-1}$, 0.85 $cm^3 \cdot g^{-1}$ and 198.4 Å, respectively. Compared with mesoporous γ-Al_2O_3, the specific surface area, pore area, pore volume and average pore size of TiO_2@Al_2O_3 were all decreased, due to the partial loading of nano TiO_2 particles on the pore surface of mesoporous γ-Al_2O_3, and the pore structure shrinks.

Table. 1. Results of Material pore structure measurement

sample	specific surface area	pore area	pore volume	average pore size
unit	$m^2 \cdot g^{-1}$	$m^2 \cdot g^{-1}$	$cm^3 \cdot g^{-1}$	Å
TiO_2	76.5	85.1	0.33	153.2
γ-Al_2O_3	185.1	205.1	1.06	206.5
TiO_2@Al_2O_3	152.1	170.7	0.85	198.4

2.2. Kinetics of catalysts

A batch reactor was constructed to evaluate the performance of the catalyst [14], as shown in Fig. 3. The heat source is provided by external circulation heating, and the pressure is controlled by the gas in the cylinder and backpressure valve. The operating temperature of reactor is 273-433 K, and the operating pressure is 100-600 kPa, and the stirring speed is set as 100 $r \cdot min^{-1}$. The reactor has

automatic data acquisition system, the temperature, pressure, stirring speed and other parameters can be recorded in real time. A certain concentration of urea solution is added into the reactor, and then the catalyst particles are added. The product gas is blown out by nitrogen gas, sent together into the infrared flue gas analyzer to measure the concentration of the product gas. The steam tracing is installed on the product gas pipeline to prevent reverse crystallization blockage of the product gas.

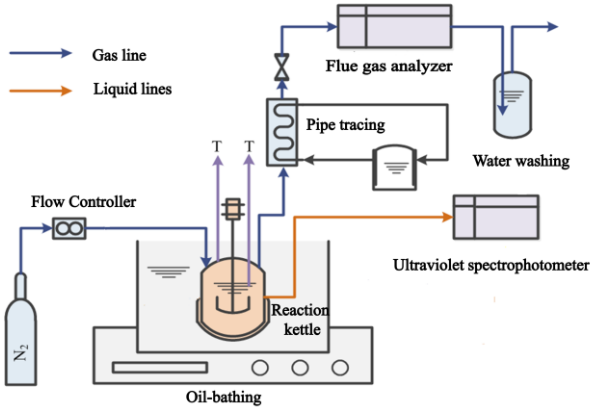

Fig. 3. Batch reactor diagram

The urea chromogenic solution has the maximum absorbance at the wavelength of 430 nm, and there is a good linear relationship between the urea concentration and absorbance [15]. The residual urea solution was diluted and mixed with 5 mL DMAB ethanol solution and 15 mL deionized water, and then the absorbance of the residual urea solution was measured in the UV spectrophotometer, which was compared with the standard absorbance curve to obtain the urea concentration. The absorbance curve of the standard urea solution is shown in eq. (3):

$$y = 31.1429x + 0.023 \tag{3}$$

Where y is the urea concentration, wt%; x is the absorbance at the wavelength of 430 nm.

Five catalysts with different Ti/Al molar ratios were prepared, and the metal elements were measured by ICP (Inductively Coupled Plasma), as shown in Table. 2, and the highest Ti/Al molar ratio was 23.35%. The urea hydrolysis with different catalysts was further tested at the temperature of 373 K. The urea decomposition rate was 30.4% when using the mesoporous γ-Al_2O_3 as catalyst, and its catalytic effect was obviously improved after loading TiO_2. When the molar ratio of Ti to Al was 5.5%, the urea decomposition rate reaches its maximum value of 35.7%, which was increased by 5.3% compared to mesoporous γ-Al_2O_3. Therefore, the optimal molar ratio of TiO_2 to mesoporous γ-Al_2O_3 is 1:10, and the increasing of loading amount of TiO_2 will lead to a decrease of the specific surface and pore blockage of the catalyst, resulting in a decrease of the exposure efficiency of active sites, and a decrease of urea decomposition rate [16].

Table. 2. Catalyst molar ratio and hydrolysis efficiency

Catalyst	TiO_2	Al_2O_3	molar ratio	hydrolysis efficiency
unit	mol	mol	%	%
Al_2O_3	0	10	-	30.4
TiO_2@Al_2O_3-0.05	0.5	10	2.9	32.7
TiO_2@Al_2O_3-0.1	1	10	5.5	35.7
TiO_2@Al_2O_3-0.2	2	10	9.4	35.1

$TiO_2@Al_2O_3$-0.4	4	10	23.35	32.8

The intrinsic kinetic equation of urea hydrolysis reaction can be simplified as follows [12]

$$-r_{ur} = -dc_{ur} / dt = kc_{ur}^{n} \quad (4)$$

Where r_{ur} is rate of decrease of reactants, $mol \cdot L^{-1} \cdot s^{-1}$; c_{ur} is molar concentration of reactants, $mol \cdot L^{-1}$; n is reaction order; k is the rate constant of reaction, which satisfies Arrhenius' law, as shown in eq. (5):

$$k = A\exp[-E / RT] \quad (5)$$

Where R is gas constant; T is temperature; K, A is pre-exponential factor, s^{-1}; E is activation energy, $kJ \cdot mol^{-1}$.

At present, the commonly used catalyst for urea hydrolysis is diammonium hydrogen phosphate ($(NH_4)_2HPO_4$), which is a water-soluble liquid catalyst, while the $TiO_2@Al_2O_3$ is a water-insoluble solid catalyst [17]. The catalytic activity of different catalysts was examined in the batch reactor under the conditions, the pressure is 600 kPa, the initial urea solution concentration is 40wt%, and the amounts of catalysts are 1 g, and the stirring speed is 100 $r \cdot min^{-1}$. The variation curves of residual urea solution concentration with time were measured at different conditions of catalyst and temperature, as shown in Fig. 4. With the increase of reaction temperature, the concentration of residual urea solution decreases and the urea decomposition rate is increased. Under the same temperature and reaction time, the decomposition rate of urea catalyzed by $TiO_2@Al_2O_3$ was the highest.

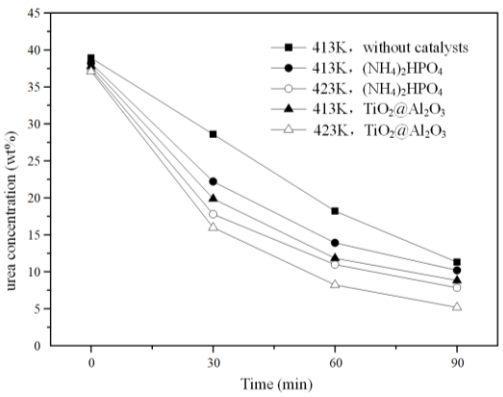

Fig. 4. The variation curves of urea solution concentration with time under different temperatures

The hydrolysis reaction rate constants were calculated from the variation curves of urea solution concentration with time, and then substituted the reaction rate constants at different temperatures into eq. (4) and fitted the pre-exponential factor and the activation energy [18], as shown in Fig. 5. The pre-exponential factor and activation energy of urea hydrolysis reaction catalyzed by different catalysts are shown in Table. 3. As we can see that the addition of catalysts can promote intermolecular collisions and reduce the activation energy of hydrolysis reaction.

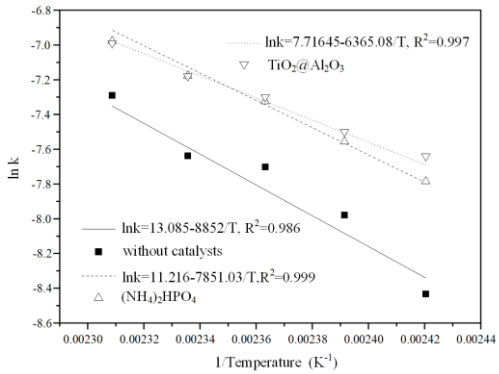

Fig. 5. Activation energy and pre-exponential factors of urea catalytic hydrolysis

Table. 3. Pre-exponential factor and activation energy of urea hydrolysis reaction

	pre-exponential factors (s^{-1})	activation energy ($kJ \cdot mol^{-1}$)
without catalysts	481666.7	73.6
$(NH_4)_2HPO_4$	74329.3	65.3
$TiO_2@Al_2O_3$	2244.9	52.9

The activity stability of $TiO_2@Al_2O_3$ as hydrolysis catalyst was tested. The catalyst particles were collected after evaporating the urea solution at 413 K and 150 kPa, and then were added into the fresh urea solution. After 60 minutes of reaction, the residual urea solution concentration was detected, and the above process were repeated for 5 times, the urea solution concentrations were 11.8%, 11.9%, 12.0%, 12.0%, and 12.1%, respectively. It can be seen that, the concentrations of residual urea solution were basically unchanged after 5 cycles, which indicated that the solid catalyst was not decomposed or had other side reactions in the urea hydrolysis reaction, and the activity is relatively stable.

2.3. Analysis of catalytic mechanism

The main components of urea solutions were detected by ^{1}H and ^{13}C NMR. The results of ^{1}H NMR are shown in Fig. 6a, and the peak position of urea solution was 4.72 ppm, which is the primary amine N-H_2 signal peak. A new peak was appeared at 5.76 ppm after hydrolysis, which might be the secondary amine N-H signal peak derived from biuret. There was no significant change of peak position and intensity of N-H signal with the addition of catalyst compared to that without catalysts. The results of ^{13}C NMR tests are shown in Fig. 6b, and the signal peak for the C=O double bond appeared at 162.8 ppm. A weak peak appeared near 157.4 ppm after the addition of catalyst, which might be derived from the intermediates such as ammonium carbamate or cyanuric acid. The intensity of C=O signal weakens after adding the catalyst, indicating that more urea has been decomposed, and the addition of catalyst is beneficial to improve the decomposition of urea.

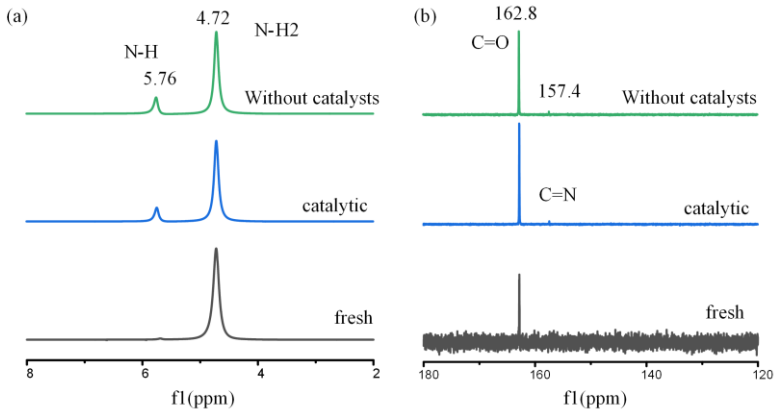

Fig. 6. ^{1}H and ^{13}C NMR test results

The rate determining step of urea hydrolysis reaction is the process of generating ammonium carbamate, and the increasing of alkalinity is beneficial to promote the carbamate dissociation and ammonia production. The adsorption energy of water molecules on the catalytic surface sites was calculated by DFT, and the adsorption energy of Al_2O_3 for water molecules is -0.55 eV, while on TiO_2@Al_2O_3, it is -0.64 eV. According to the XPS (X-ray photoelectron spectroscopy) characterization results, the electronegativity of Al atoms is regulated by Ti atoms, which makes it easier for oxygen atoms on water molecules to adhere to the TiO_2@Al_2O_3 surface. Compared with non-catalytic conditions, the water molecules are more easily dissociated into H and OH radicals on the catalyst surface to participate in the urea hydrolysis reaction.

The catalytic mechanism of TiO_2@Al_2O_3 on urea hydrolysis is as follows: Firstly, the electronegativity of Ti atoms on the surface of TiO_2@Al_2O_3 is regulated by Al atoms, which makes it easier for water molecules to adsorb on Ti sites, and the electrons of O atoms migrate towards Ti atoms. Dissociation of water molecules occurs when absorbing 0.602 eV of energy, and active hydroxyl groups and protons appear in the solution, which make it easier for urea molecules to form amino acid ester intermediates. And then the ammonium carbamate decomposes faster after absorbing heat, generating ammonia and carbon dioxide. These can be simplified to the following reaction eq. (6)-(10):

$$H_2O \rightarrow H^+ + OH^- \quad (6)$$

$$NH_2CONH_2 + OH^- \rightarrow NH_2COOHNH_2^- \quad (7)$$

$$NH_2COOHNH_2^- + H^+ \rightarrow NH_3 + NH_2COOH \quad (8)$$

$$NH_2COOH + H_2O \rightarrow NH_3 + H_2CO_3 \quad (9)$$

$$H_2CO_3 \rightarrow H_2O + CO_2 \quad (10)$$

3. Pilot test of urea catalytic hydrolysis

In order to simulate the transfer process of industrial reactor, a pilot plant of urea catalytic hydrolysis was built [19], as shown in Fig. 7. The reactor volume is 220 L, the urea solution concentration is 50wt%, the designed ammonia production rate is 12 kg/h, and the operating pressure is 0.6 MPa. The kettle reactor can be operated continuously with good full mixing and heat transfer characteristics, which can ensure the uniformity of temperature and concentration distribution.

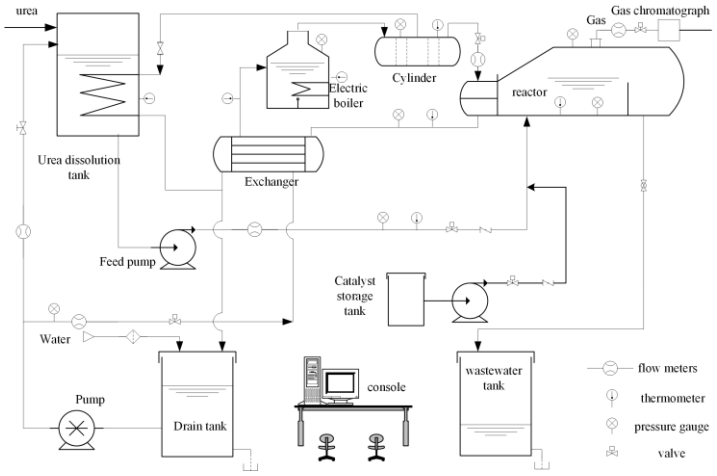

Fig. 7. Pilot test plant of urea catalytic hydrolysis

The softened water in the drain tank is sent to the urea dissolution tank through a feedwater pump to mix with urea particles to prepare for urea solution, and the other way is preheated by a heat exchanger and then sent to the electric boiler to generate high-temperature steam. The urea solution is fed into the hydrolysis reactor by the feed pump, and hydrolyzed to produce ammonia gas. The heat required for hydrolysis reaction is provided by steam, and the steam changes to saturated water which is cooled down in the heat exchanger and then returned to the drain tank. The product gas is discharged from the top of the reactor, and the residual liquid is sent to the wastewater tank for reprocessing. All instrumentation data is sent to the control console for analysis and processing. A catalyst feed circuit including catalyst storage tank, feed pumps, switching valves, and check valves are added to feed catalyst solution to the feed circuit of urea solution.

The urea catalytic hydrolysis was carried out on the pilot plant with the catalysts of diammonium hydrogen phosphate and $TiO_2@Al_2O_3$. The 15.4 L 50wt% diammonium hydrogen phosphate solution was mixed with the feed urea solution and fed into the hydrolysis reactor. And the 20 kg solid catalysts $TiO_2@Al_2O_3$ particles were mixed with deionized water to form a suspension, then added to the feed urea solution through the catalyst storage tank.

The experimental conditions are shown in Table. 4. The opening of the regulator valve at the reactor outlet was kept unchanged at different conditions, so that the product gas flow rates were basically equal, and the reaction temperatures were adjusted. It can be seen that after adding catalysts, the same product gas flow rate can be achieved at a lower reaction temperature.

Table. 4. Experimental conditions of urea catalytic hydrolysis

Case		1	2	3	4	5
without catalysts	Ammonia production rate ($kg \cdot h^{-1}$)	32.2	36	44.5	50.2	52.7
	Temperature (K)	423	425	428.5	430.5	431.5
$TiO_2@Al_2O_3$	Ammonia production rate ($kg \cdot h^{-1}$)	31.8	35.7	44.2	49.5.	51.9
	Temperature (K)	412	414	418	420	421
$(NH_4)_2HPO_4$	Ammonia production rate ($kg \cdot h^{-1}$)	32.5	35.2	44.1	49.2	51.4
	Temperature (K)	415	418	423	427	428.5

The product gas was sent into the gas chromatograph to detect the concentration of each component in the gas phase, as shown in Fig. 8. It can be seen that the chromatographic curves showed three peaks at similar residence times, corresponding to carbon dioxide, ammonia and water vapor. The area surrounded by each peak represents the volume fraction of each component. The volume fractions of each component in the gas phase did not change significantly after adding the liquid and solid catalysts, which indicated that the catalysts were not consumed and no side reaction occurred during the reaction process, and the volume fractions of each component in the product gas was only determined by the concentration of the feed urea solution according to the material balance.

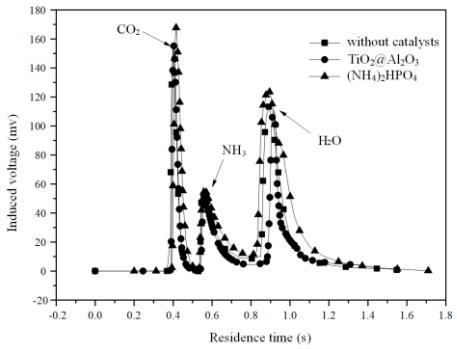

Fig. 8. Chromatographic curves of gaseous products of urea catalytic hydrolysis

The gas and liquid phases reached dissolution equilibrium at the phase interface in the hydrolysis reactor. The gas-liquid equilibrium of solvent H_2O conformed to the modified Lewis-Randall equation, and the gas-liquid equilibrium of ammonia and carbon dioxide conformed to the modified Herry equation [19]. The concentrations of each component in the liquid phase were calculated according to the detected concentration of the products in the gas phase and the gas-liquid equilibrium equations, as shown in Table. 5. The concentrations of ammonia and carbon dioxide in the liquid phase are mainly determined by the solubility, the ammonia concentration in the liquid phase is increased while it is decreased of carbon dioxide after the addition of catalyst. Besides, the concentration of urea and ammonium carbamate is decreased after adding the catalyst, indicated that the catalysts can promote the decomposition of urea and ammonium carbamate.

Table. 5. Concentration of liquid-phase components of urea catalytic hydrolysis

molarity	Urea ($mol \cdot L^{-1}$)	$NH_3 \times 10^{-3}$ ($mol \cdot L^{-1}$)	$CO2 \times 10^{-5}$ ($mol \cdot L^{-1}$)
Without catalysts	1.85	2.7	1.222
$TiO@Al_2O_3$	1.4	2.9	1.219
$(NH_4)_2HPO_4$	1.68	3.28	1.217

The ammonia production rates at different temperatures were calculated according to the product gas flow rates and detection data of gas-phase concentration, as shown in Fig. 9. It can be seen that the ammonia production rates were increased after adding catalysts, and the ammonia production rate of the solid catalyst $TiO_2@Al_2O_3$ was larger than that of the liquid catalyst diammonium hydrogen phosphate at the same temperature.

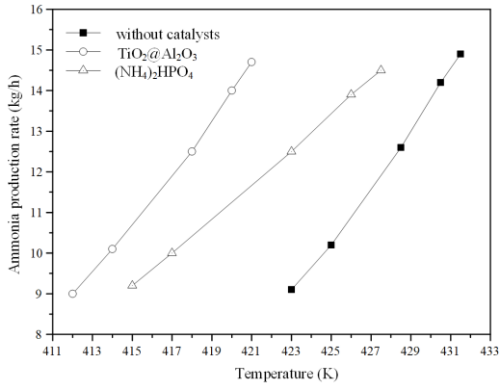

Fig. 9. Curves of ammonia production rate with temperature

Previous studies have shown that the urea hydrolysis to ammonia is a liquid-phase slow reaction [20], and the ammonia production rate is controlled by kinetics, it is not affected by the mass transfer process. The dimensionless number *M* [21] of the hydrolysis reaction is shown in Fig. 10. The dimensionless number *M* increased after the addition of the solid catalyst, indicating that the solid catalyst increased the chemical reaction rate of urea hydrolysis. From the fitting curve of the dimensionless number, it can be seen that the dimensionless number *M* is less than 0.06 in the temperature interval of the hydrolysis reaction, so the ammonia production of urea hydrolysis under solid catalytic condition is still a liquid-phase slow reaction, and the ammonia diffusion rate is much larger than the intrinsic chemical reaction rate, and the ammonia production rate is still controlled by the intrinsic reaction kinetics.

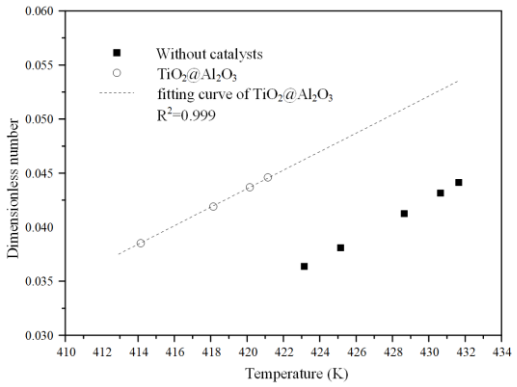

Fig. 10. Dimensionless number of catalytic hydrolysis of urea

The urea hydrolysis reaction is endothermic, and the required heat is provided by the steam in the coil, with parameters of 1.0 MPa/453 K. The energy consumptions of ammonia production of urea catalytic hydrolysis were calculated according to the steam consumption at different conditions, as shown in table. 11. The heat required for urea hydrolysis consists of three parts [22], the first is the heat absorption of the chemical reaction, the second is the heat required for heating the urea solution to the reaction temperature, and the third is the latent heat of vaporization of the excess water. With the addition of catalysts, the hydrolysis reaction temperature is reduced under the same ammonia production demand, and the second part of heat is reduced, so the energy consumption of ammonia

production from catalytic hydrolysis is lower than that from urea hydrolysis without catalysts. On the other hand, the chemical reaction heat and the latent heat of water gasification account for the main share in the three parts, thus the energy consumption of ammonia production by catalytic hydrolysis is only reduced by about 3%.

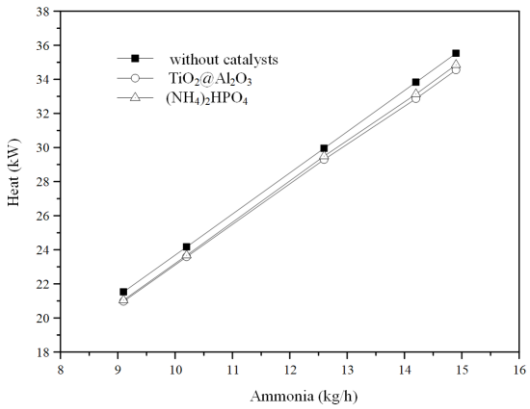

Fig. 11. Energy consumption for ammonia production of urea catalytic hydrolysis

The existing hydrolysis reactor has the function of reaction zone and ammonia buffer zone. When the load changes, the outlet valve increases, the pressure in the reactor is decreased, and the stored ammonia can quickly respond to the change in ammonia demand in generally 1-3 seconds. However, the capacity of the ammonia buffer zone is limited, and it cannot support the new load demand for a long time, thus it is necessary to regulate the feed urea solution valves and the heating steam valves to achieve a stable response to variable loads. Therefore, the variable load response time of the urea hydrolysis reactor is defined as follow: the time elapsed from the moment the reactor receives an ammonia change command from the SCR zone to the moment the temperature and pressure in the reactor stabilize.

The response times of load change in ammonia production at different conditions were counted and are shown in Fig. 12. It can be found that the variable load response time of hydrolysis reactor was decreased obviously after adding catalysts, and the variable load response times of liquid and solid catalysts were basically equal. The results indicated that the catalyst can improve the chemical reaction rate, thereby reducing the thermal inertia and the temperature rise and fall time of the hydrolysis solution, and improving the variable load response rate.

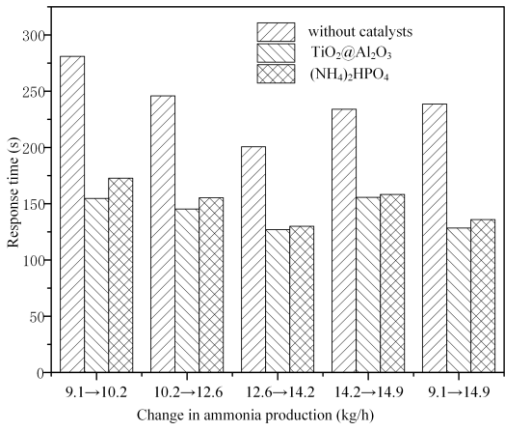

Fig. 12. Variable load response time of urea catalytic hydrolysis reactor

4. Conclusions

The bimetallic solid catalyst $TiO_2@Al_2O_3$ was synthesized by loading TiO_2 on the mesoporous γ-Al_2O_3, and it has abundant active sites and a large specific surface area. The effect of synthesis conditions on the surface structure and chemical properties of $TiO_2@Al_2O_3$ catalyst was characterized by Raman spectroscopy and TEM, and the optimal molar ratio of TiO_2 to mesoporous γ-Al_2O_3 was selected to be 1:10. The DFT calculations proved that the Al atoms on the surface of $TiO_2@Al_2O_3$ could regulate the electronegativity of Ti atoms , and promote the dissociation of water molecules adsorbed on the metal oxides surface, to form two types of active site such as terminal hydroxyl and active proton. The hydroxyl reacts with ammonium carbamate, the intermediate product during urea hydrolysis, to generate ammonia, which makes the overall urea hydrolysis reaction to proceed in a positive direction.

The kinetic and thermodynamic properties of the urea catalytic hydrolysis were investigated on a batch reactor and a continuous operation pilot plant, and the influences of different catalysts on the hydrolysis temperature, energy consumption and variable load response time were compared. The addition of solid catalyst $TiO_2@Al_2O_3$ reduced the activation energy of the hydrolysis reaction from 73.6 kJ·mol^{-1} to 52.9 kJ·mol^{-1}, and the urea conversion was achieved to nearly 87.2% at 413 K, 600 kPa and 60 min reaction time. The solid catalysts are able to increase the hydrolysis reaction rate and reduce the hydrolysis reaction temperature, and the catalyst activity is still stable after 5 cycles. In the continuous operating reactor, the urea catalytic hydrolysis to ammonia with the addition of solid catalyst is still a slow reaction in the liquid phase, due to the diffusive rate of ammonia is much greater than that of the intrinsic chemical reaction rate. The energy consumption of ammonia production in catalytic hydrolysis was about 1-3% lower than that of ordinary hydrolysis. The variable load response time of the hydrolysis reactor was significantly reduced after the addition of catalyst, and the variable load response times of catalytic hydrolysis were less than 5 min.

Acknowledgments

This work is sponsored by the Shaanxi Province Key R&D Program(Contract NO.:2024GX-YBXM-458), Science and Technology Project of China Huaneng Group (Contract NO.: HNKJ22-H34).

Nomenclature

r_{ur}	rate of decrease of reactants, mol·L^{-1}s^{-1}
c_{ur}	molar concentration of reactants, mol·L^{-1}
t	time, s
R	gas constant
T	temperature, K
K	pre-exponential factor, s^{-1}
A	pre-exponential factor, s^{-1}
E	activation energy, kJ·mol^{-1}

M dimensionless number

References

[1] YAO, X., *et al*., Characteristics of urea hydrolysis equipment for flue gas denitration, *Proceeding of the CSEE, 33*(2013),14, pp. 38-43

[2] Sahu, J.N., *et al.*, Response surface modeling and optimization for production of ammonia from urea in a batch reactor, *Chemical Engineering*, (2009), 4, pp. 462-470

[3] Mahalik, K., *et al.*, Statistical modeling and optimization of hydrolysis of urea to generation ammonia for flue gas conditioning, *Journal of Hazardous Materials, 182*(2010), 1, pp. 603-610

[4] ZHENG, P., *et al*., Design guidelines for urea hydrolysers for ammonia demand of the SCR DENOX project in coal-fired power plants, *Energy, 7*(2013), 1, pp. 127-132

[5] Young, D.C., Transporting urea for quantitative conversion into ammonia, United states patent: 5252308, 1993-10-12

[6] Mahalik, K., *et al.*, Equilibrium studies on hydrolysis of urea in a semi-batch reactor for production of ammonia to reduce hazardous pollutants from flue gases, *Journal of Hazardous Materials, 164*(2010), pp. 659-664

[7] Yang, W., *et al.*, Catalytic performance of zeolites on urea thermolysis and isocyanic acid hydrolysis, *Industrial & engineering chemistry research*, *50*(2013),13, pp. 7990-7997

[8] Eichelbaum, M., *et al.*, The impact of urea on the performance of metal exchanged zeolites for the selective catalytic reduction of NOx: Part I. Pyrolysis and hydrolysis of urea over zeolite catalysts, *Applied Catalysis B: Environmental*, *97*(2010), 1, pp. 90-97

[9] Guo, C., *et al.*, Rapid in situ synthesis of MgAl-LDH on η-Al2O3 for efficient hydrolysis of urea in wastewater, *Journal of Catalysis*, *395*(2021), pp. 54-62

[10] Fan, X., *et al.*, Plasma-catalytic hydrolysis of urea for ammonia production: Optimization and kinetic study, *Industrial & Engineering Chemistry Research*, *60*(2021), 48, pp. 17480-17488

[11] Kuntz, C., *et al.*, Deposition and decomposition of urea and its by-products on TiO2 and VWT-SCR catalysts, *International Journal of Heat and Fluid Flow, 95*(2022)

[12] Meguerdichian, A.G., *et al.*, Synthesis and electrocatalytic activity of ammonium nickel phosphate, [NH4] NiPO4·6H2O, and β-nickel pyrophosphate, β-Ni2P2O7: catalysts for electrocatalytic decomposition of urea, *Inorganic Chemistry, 57*(2018), 4, pp. 1815-1823

[13] Bernhard, A.M., *et al.*, Catalytic urea hydrolysis in the selective catalytic reduction of NOx: catalyst screening and kinetics on anatase TiO2 and ZrO2, *Catalysis Science & Technology, 3*(2013), 4, pp. 942-951

[14] Sahu, J.N., *et al.*, Equilibrium and kinetic studies of in situ generation of ammonia from urea in a batch reactor for flue gas conditioning of thermal power plants, *Industrial & Engineering Chemistry Research, 48*(2020), 3, pp. 2705-2712

[15] Vander, K.S., *et al.*, Multiparameter determination of thin liquid urea-water films, *Applied Sciences-Basel, 11*(2021), 19

[16] Zheng, S., *et al*., On the roles of humidification and radiation during the ignition of ammonia–hydrogen–air mixtures, *Combustion and Flame*, *254*(2023), 112832

[17] Shen, S., *et al.*, Catalytic hydrolysis of urea from wastewater using different aluminas by a fixed reactor, *Environmental Science and Pollution Research*, *21*(2014), pp. 12563-12568

[18] Ying, W., *et al.*, In situ growth of highly active MgAl layered double hydroxide on η-Al2O3 for catalytic hydrolysis of urea in wastewater. *Catalysis Letters*, *148*(2018), pp. 1893-1903

[19] Zhang, X.Y., *et al.*, Experimental study on urea hydrolysis to ammonia for gas denitration in a continuous tank reactor, *Energy*, (2017), 126, pp. 677-688

[20] Wang, S., Simulation research on absorption refrigeration system based on NH3-H2O-LiBr vapor-liquid equilibrium calculation model, *Thermal Science 26*(2022) pp. 1825-1840

[21] Ma, Y., *et al.*, Urea-related reactions and their active sites over Cu-SAPO-34: Formation of NH3 and conversion of HNCO, *Applied Catalysis B: Environmental, 227*(2018), pp. 198-208

[22] Wang, D, *et al.*, A review of urea pyrolysis to produce NH3 used for NOx Removal, *Journal of Chemistry*, (2019), pp. 1-11

Submittes: 28.05.2024.
Revised: 30.07.2024
Accepted: 05.08.2024.